JOURNAL OF APPLIED ELECTROCHEMISTRY 20 (1990) 235–239

Morphological changes in the electrodes of phosphoric acid fuel cells operating under open circuit voltage conditions

V. ALDERUCCI, E. PASSALACQUA, N. GIORDANO

CNR Institute for Transformation and Storage of Energy, Salita S. Lucia sopra Contesse 39, 98126 S. Lucia, Messina, Italy

P. L. ANTONUCCI

University of Reggio Calabria, Faculty of Engineering, Via Cuzzocrea, 48, 89100 Reggio Calabria, Italy

F. PARMIGIANI, N. RICCI

Materials Department CISE Tecnologie Innovative S.p.A., Via Reggio Emilia, 39, 20090 Segrate, Milano, Italy

Received 11 January 1989; revised 26 May 1989

This paper reports the experimental evidence for morphological changes that occur at the electrodes of phosphoric acid fuel cells (PAFC) under very severe (OCV) conditions. In addition, the dissolution of Pt-supported crystallites in H_3PO_4 is demonstrated by Transmission Electron Microscopy (TEM) confirming previous results already reported in the literature. Finally, the experimental data are discussed on the basis of an analysis of the reaction rates and models for the corrosion mechanism is postulated.

1. Introduction

As is well known, the performance and endurance of phosphoric acid fuel cell gas-diffusion electrodes critically depends on their morphology and their physical structure [1] and this may change during operation, drastically reducing the efficiency of the systems. Possible sources of the progressive decrease of the electrode efficiency can arise from carbon corrosion effects [2], improper electrolyte management [3] and incorrect sintering processes of the catalysts. Some studies of this subject have been reported, mainly devoted to topical problems such as changes in the total amount of Pt, the spatial distribution of Pt crystallites, carbon corrosion mechanisms and Pt crystallite sintering during long term PAFC operation [4–9]. However, information is lacking concerning weight loss, catalyst pore size distribution and correlation between pore size and PAFC electrode wettability.

The aim of this paper is to answer these latter questions by means of a microstructural study of gas-diffusion electrodes exercised for different operating times (1, 5, 24, 120, 296 h) under severe conditions, namely, OCV (1 V), 99% H_3PO_4 at 180° C.

2. Experimental

The electrodes were prepared from carbon paper (Stackpole PC 206) wetproofed with a FEP (polytetrafluoroethylene–propylene) solution, dried at 70° C and sintered at 340° C for 15 min. The catalyst ink was prepared by mixing and stirring at 50 to 60° C, for 15 min, 62 ml H_2O, 2.2 ml Teflon solution (51% w/w) and 3 g 10% Pt/C catalyst. Isopropyl alcohol (23 g) was added to the catalyst ink and the flocculate was screen printed (Argon Modular 2) on the carbon paper. The electrode was dried in air in two steps at 120° C for 1 h and at 230° C for 30 min, and then sintered at 340° C. The final content of PTFE was 40% and the Pt content was 0.5 mg cm^{-2}. Corrosion tests of up to 300 h were performed in atmospheric conditions with the keeping electrodes in 99% H_3PO_4 (J.T. Baker), in an all-Teflon holder at 180° C. The rest potential of the electrodes, periodically checked with an Amel model 551 potentiostat, was 1 ± 0.015 V. The H_3PO_4 content in the catalytic layer ($V_{H_3PO_4}$) was determined gravimetrically. The weight losses (ΔW) were determined after 1, 5, 24, 120 and 296 h, respectively, following complete elimination of the H_3PO_4 by a washing procedure with methanol. The pore volume and pore size distribution of the electrodes were measured by the mercury intrusion technique with a porosimeter (Carlo Erba model 2000). Phosphoric acid occupation (PAO), taken as an index of the wettability of the electrodes [11, 12], was determined using the following equations

$$V_p = V_s\left(\frac{a}{a+b}\right) + V_{cl}\left(\frac{b}{a+b}\right) \qquad (1)$$

where V_{cl} is the pore volume of the catalytic layer,

Table 1. Summary of main characteristics of electrodes

Sample	*Catalyst density ($mg\,cm^{-2}$)*	*Thickness (mm)*	*Gas permeability ($cm^3\,min^{-1}\,cm^{-2}\,mm\,H_2O^{-1}$)*	*Total pore volume ($mm^3\,g^{-1}$)*	*Macropore volume ($>0.4\,\mu m$) ($mm^3\,g^{-1}$)*	*Micropore volume ($\leqslant 0.4\,\mu m$) ($mm^3\,g^{-1}$)*
59-3C6	5.0	0.61	0.08	487	247	240
59-3C7	5.2	0.43	0.10	711	300	411
62-2	5.5	0.52	0.08	441	130	311
62-2A	5.4	0.56	0.07	556	132	424

V_p is the pore volume of the electrode, V_s is the pore volume of the carbon paper, $V_{H_3PO_4}$ is the volume of H_3PO_4 adsorbed, a is the density of the carbon paper, and b is the density of the catalytic layer.

2.1. *Transmission electron microscopy*

Transmission electron microscopy was performed using a STEM apparatus (Jeol CX20) whose ultimate spatial resolution is 0.5 nm.

To allow a uniform distribution of the Pt crystallites, the catalytic layer was first dispersed in isopropyl alcohol and then deposited and dried on a TEM support comprising a Cu grid covered with a carbon film of a few tens of nanometres in thickness.

3. Results

The main parameters of the electrodes tested are given in Table 1; the catalyst layer losses ΔW, expressed in $mg\,cm^{-2}$, as a function of time are shown in Fig. 1. The increase in ΔW in the first part of the curve is common to all samples. At the end of the test, the asymptotic values of ΔW are in the range 0.5 to 0.8 $mg\,cm^{-2}$, which correspond to an overall loss of 10 to 16% w/w (Table 1).

In a parallel manner the PAO values vary from 16 to 45% for the fresh electrodes up to 55 to 93% for the spent electrodes (Fig. 2), reflecting a progressive filling of the electrode porous structure by the electrolyte. The quasi-steady-state PAO values are reached after 120 h of test. Figure 3 shows the morphological evolution of the electrodes in terms of pore volume and size distribution. A gradual increase in the total pore volume is observed (Fig. 3a). This variation appears to be due to a progressive increase in the volume of the micropores (up to 0.4 μm, Fig. 3b), whereas macropore diameters (> 0.4 μm, Fig. 3c) remained unchanged.

Figure 4 shows a selection of TEM micrographs taken at different times (fresh, after 5 h and after 290 h of operation). The dark spots are due to platinum clusters which lie on carbon agglomerates (grey areas). Unfortunately, a clear distinction between carbon and Teflon is not possible. It is seen that the fresh sample has a homogeneous distribution of Pt crystallites with an average size of 6.0 to 7.5 nm, while the carbon agglomerate sizes are about 0.5 μm. The 5 h sample does not display significant changes in the morphology of the particles, whereas a detectable decrease in the number of Pt particles is observed. This phenomenon is much more marked for the 290 h sample. The disappearance of Pt is evident by comparing the metal particle densities reported in Fig. 4a–c. A concomitant coarsening of Pt crystallites, up to dimensions of 18 nm, is also observed.

4. Discussion

Present results indicate that significant structural and absorptive changes occur during the exercise of typical PAFC electrodes. The ΔW–time results reported here agree with previous data [10], confirming that, at constant potential, the corrosion process is initially

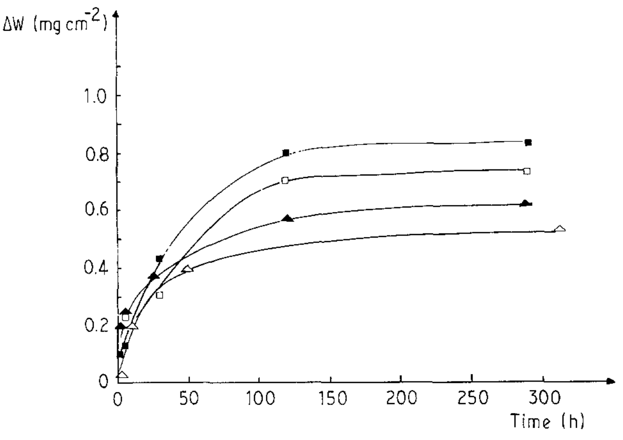

Fig. 1. Electrode weight losses ($mg\,cm^{-2}$) as a function of time: Samples, 593C-6 (■), 593C-7 (□), 62-2 (▲), 62-2A (△).

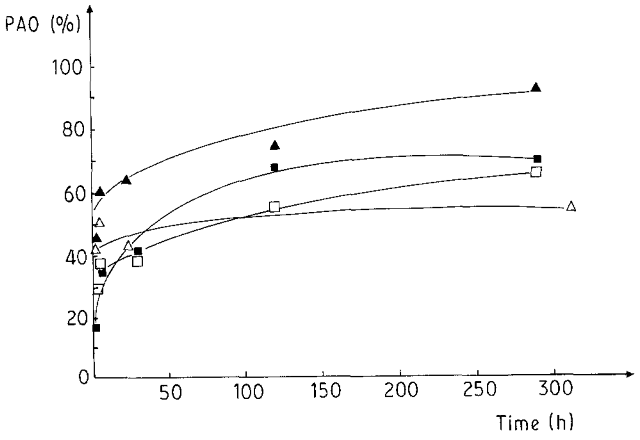

Fig. 2. Electrode phosphoric acid absorption (%) as a function of time. Symbols as in Fig. 1.

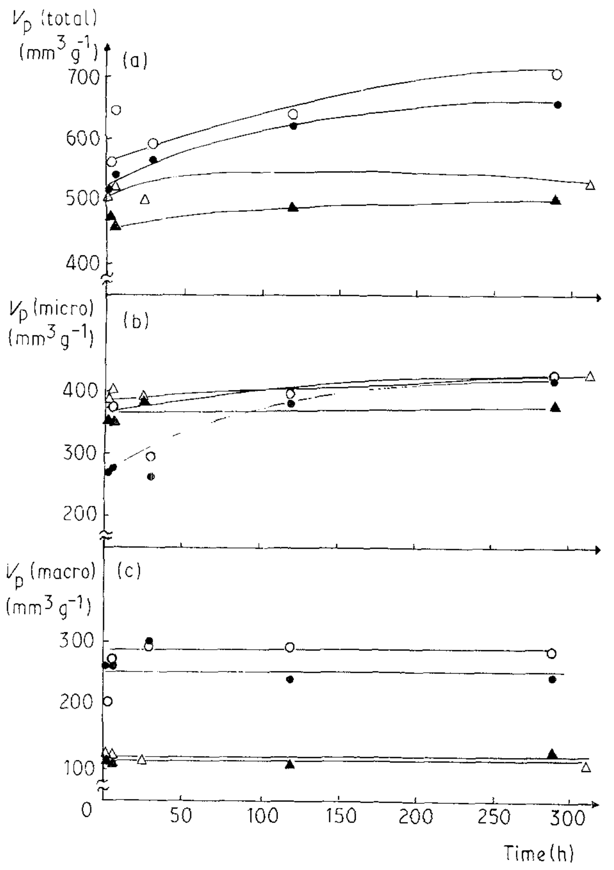

Fig. 3. (a) Total pore volume ($mm^3 g^{-1}$) as a function of time. (b) Micropores volume ($mm^3 g^{-1}$) as a function of time. (c) Macropores volume ($mm^3 g^{-1}$) as a function of time. Symbols as in Fig. 1.

intense whereas it decreases quickly as the operating time increases. As is well established [10], carbon corrosion decreases sharply with time, the process being caused by a progressive removal of the more disordered fractions of carbon and then by attack at micropores and dislocations [13] resulting in CO_2 evolution as a consequence of the reaction of the electrochemical oxidation of carbon in aqueous solution, described by $C + 2H_2O \rightarrow O_2 + 4H^+ + 4e$ [14–18], where, as is well known, the water content of the H_3PO_4 constitutes the corrosion reactant. Also, there is a concomitant formation of oxygenated surface groups, whose rate of growth decreases as CO_2 evolution becomes the major process [19]. In this regard, the observed increase in wettability at the onset of the experiment (see Fig. 2) can be explained by an increased hydrophilicity, in parallel with the formation of oxygenated complexes [19, 20].

To account for the present differences in the experimental functions reported in Figs 1 and 2, we suggest that the process leads first to a preferential evolution of CO_2 (as denoted by the relatively greater increase in ΔW, Fig. 1) than to an accumulation of surface oxides, as suggested by a lower rate of increase in the PAO as a function of time. In fact the formation of surface oxides has been demonstrated to be more significant under milder conditions of oxidation (135° C) [19].

It is likely that the increase in oxygen content of the carbon (and then in its hydrophilic character) can account, almost in part, for the observed initial increase in PAO, as previously observed [20]. Nevertheless, it does not explain completely the H_3PO_4 absorption rate measured up to the first half of the test. It has been previously shown that the wettability of carbon subjected to electrochemical oxidation at 135° C remains constant, while growth of the oxygenated groups continues [15]. Thus the relationship between PAO values and surface oxide concentration appears not to be unique. In this regard, as the whole

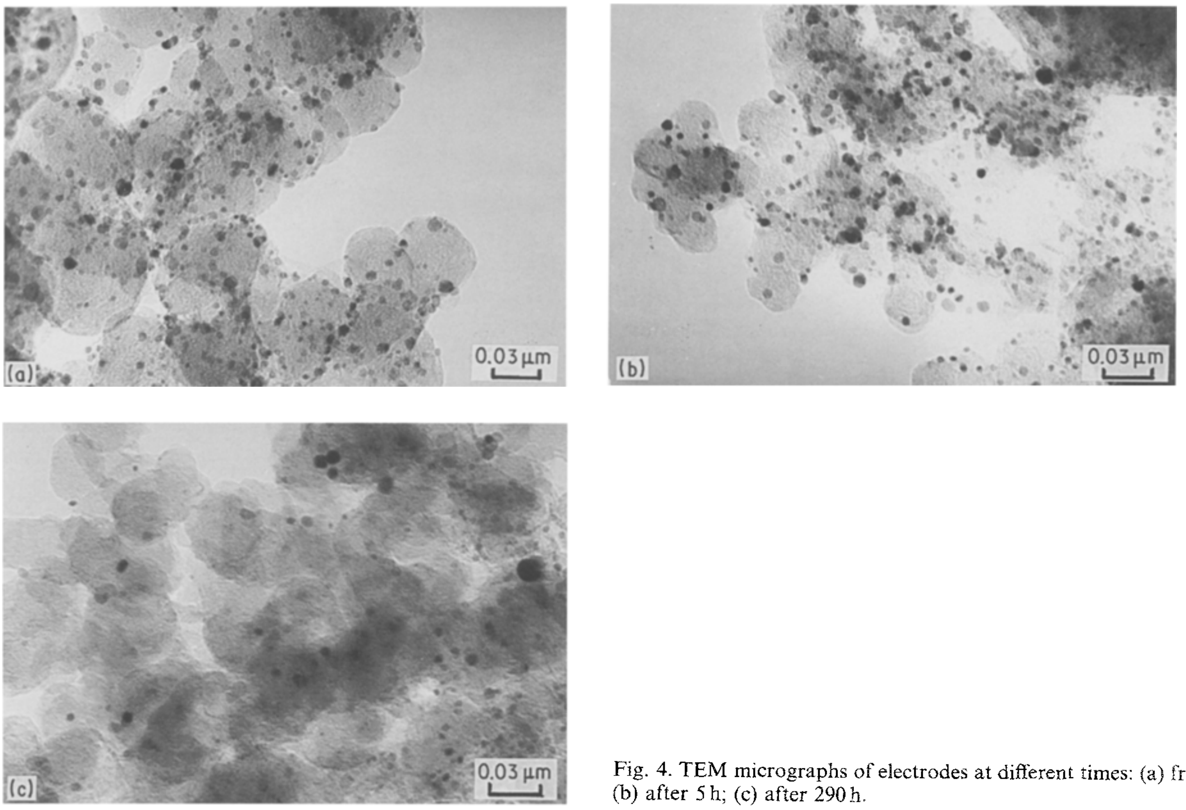

Fig. 4. TEM micrographs of electrodes at different times: (a) fresh; (b) after 5 h; (c) after 290 h.

process is also accompanied by variations in pore volumes, as shown in Fig. 3 (especially in the amount of micropores (Fig. 3b)), the contribution of the pore volume to the increased PAO values cannot be excluded.

Note that the same processes already demonstrated in case of thermal oxidation of carbon blacks [21, 22] can also explain the evolution of the porosity in the present experiments. An example is the study by Blurton *et al.* [21], who demonstrated the formation of either meso-slit pores or micropores on Fe-catalysed oxidation of carbon black. Moreover, the formation and the subsequent removal of carboxylic oxide complexes from the carbon surface after heat treatments up to 800° C open up the micropores, inducing an enhancement in the surface area and porosity [10]. A noticeable rise, both in total pore volume and microporosity, has been noticed by increased burn-off of some activated carbons [22].

The almost parallel increase in PAO and microporosity values seems then to support the hypothesis that the two phenomena are connected, that is, phosphoric acid appears to be progressively absorbed into the continuously increasing available volume generated by the corroding attack.

Although various carbon corrosion mechanisms in aqueous electrolytes have been proposed in the past [19, 23–28], a unified rate law for the corrosion process is not available. An attempt is made here by considering various adimensional reaction curves, each representing a possible rate controlling process [29]. Such expressions were derived by correlating experimental kinetic reaction data from the general equation $f(\alpha) = f(\alpha^*)$, where α is the fraction degree of conversion (corrosion), α^* is a reference value and $\tau = t_\alpha / t_{\alpha^*}$ is the adimensional reaction time (t_α and t_{α^*} are the reaction times required to reach degrees of conversion α and α^*, the latter choosen as a reference value equal to 0.25). The advantage of these equations consists in the fact that the adimensionality does not account for all variables not explicitly involved in the reaction mechanism, where in $f(\alpha)$ only is a characteristic function of the controlling step.

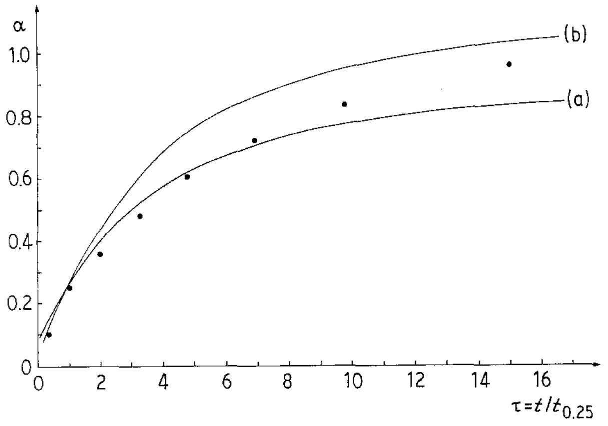

Fig. 5. Fitting of experimental corrosion rates with adimensional reaction curves: Curve a, adimensional rate expression $(1 - \alpha) = kt$ (2nd order in the solid component); Curve b, adimensional rate expression $\ln(1 - \alpha) = kt$ (internal diffusion resistance). (●) adimensional values calculated from experimental weight losses.

Weight losses were therefore evaluated in such adimensional terms, the extent of the corrosion being defined as $\alpha = W_t / W_\alpha$ where W_t is weight loss at time t and W_α is final weight loss (after completion of the 300h test). The values obtained (Fig. 5) appear to lie between the a and b adimensional curves, each related to a rate controlling mechanism. Curve a is indicative of a solid–liquid absorption process and curve b is related to a first order mechanism with respect to the solid component.

Based on the above, it is concluded that our experimental data satisfy the expression $\alpha/(1 - \alpha) = kt$ (where $\alpha = W_t / W_\alpha$ is the degree of corrosion, k is the kinetic constant of the process and t is the time), thus denoting a second order kinetic law. Accordingly, we assume one term related to the solid and the other to the liquid component concentration, just as in activated absorption in the case of gas–solid interaction (see Fig. 5, curve a), although a contribution of the internal diffusion resistance in the solid could also be envisaged (curve b), as suggested by the slight deviation from the adimensional curve at higher t. In other words, the reaction is controlled by two activated absorption steps, each characterized by a different number of active sites involved in the electro-oxidation and, as the reaction proceeds, is able to describe the reaction pattern.

5. Conclusions

The results obtained in the corrosion of typical PAFC electrodes under OCV conditions permit the following conclusions:

(i) Modifications of the structure are manifested primarily by weight losses which, initially fast, level off at longer time, reaching end values of the order of 10 to 16% of the original.

(ii) The corrosion attack causes profound modifications in the morphological characteristics of the electrodes (i.e. increase in microporosity) and concomitant significant increase in wettability, as indexed by the percentage of acid occupation.

(iii) The increase in wettability is attributed to the increased pore volume and to the progressive build-up of oxygenated groups.

(iv) The overall process may be interpreted in terms of a mechanism involving evolution of CO_2 concomitant and/or parallel with the formation of surface oxygenated groups.

(v) Using adimensional rate law expressions, it is suggested that the overall process can be described by a second order rate law, proportional to the concentration of active sites in the solid and to the concentration of the water fraction of the phosphoric acid.

(vi) The platinum dissolves almost completely after a few hundred hours in the H_3PO_4 environment.

References

[1] S. Motoo, M. Watanabe and N. Furuya, *J. Electroanal. and Interfac. Electrochem.* **160** (1984) 351.

[2] P. Stonehart and J. P. MacDonald, EPRI Report AP-57090-LD (1988).

[3] T. Mori, J. Imahashi, T. Kamo, K. Tamura and Y. Hishinuma, *J. Electrochem. Soc.* **133** (1986) 896.

[4] A. K. Kush, L. G. Christner and P. P. Yeh, Proceedings USA Fuel Cell Seminar, Tucson (1985) p. 56.

[5]. P. Bindra, S. J. Clouser and E. Yeager, *J. Electrochem. Soc.* **126** (1979) 1631.

[6] A. Honji, T. Mori, K. Tamura and Y. Hishinuma, *ibid.* **135** (1988) 355.

[7] J. Aragane, T. Murahashi and T. Odaka, *ibid.* **135** (1988) 844.

[8] A. Pebler, *ibid.* **133** (1986) 9.

[9] K. Kinoshita, K. Routsis, J. A. S. Bett and C. S. Brooks, *Electrochim. Acta* **18** (1973) 953.

[10] P. Stonehart, *Carbon* **22** (1984) 423.

[11] N. Giordano, E. Passalacqua, V. Recupero, P. Staita, V. Alderucci, R. Di Leonardo, H. Mirzaian, Z. Poltarzewski and L. Pino, Proceedings USA Fuel Cell Seminar, Chicago (1988).

[12] V. Alderucci, E. Passalacqua, V. Recupero and N. Giordano, *J. Electro chem. Soc.* (submitted).

[13] J. M. Thomas, *Adv. Catal.* **19** (1969) 293.

[14] P. Stonehart and J. Hochmuth, 'Survey on Aging on Electrodes and Electrocatalysts in Phosphoric Acid Fuel Cells', DOE/NASA Report 0176-81/3 (1981) pp. 22–29.

[15] P. L. Antonucci, F. Romeo, M. Minutoli, E. Alderucci and N. Giordano, *Carbon* **26** (1988) 197.

[16] S. S. Penner, 'Assessment of Research Needs for Advanced Fuel Cells', DOE Report ER 30060-TI (1985) pp. 40–45.

[17] A. J. Appleby, 'Corrosion in Low and High Temperature Fuel Cells – an overview', Proceedings International Corrosion Forum, paper no. 79 (1986).

[18] K. Kinoshita, 'Carbon – Electrochemical and Physicochemical Properties', Wiley, New York (1988) pp. 317–334.

[19] K. Kinoshita and J. Bett, *Carbon* **11** (1973) 237.

[20] *Idem, ibid.* **13** (1975) 405.

[21] K. F. Blurton, H. R. Kunz and D. R. Rutt, *Electrochimica Acta* **23** (1978) 183.

[22] F. Rodriguez-Reinoso, I. Rodriguez-Ramos, C. Moreno-Castilla, A. Guerrero-Ruiz and J. D. Lopez-Gonzales, *J. Catal.* **99** (1986) 171.

[23] J. Willsan and J. Heitbaum, *J. Electroanal. Chem.* **161** (1984) 93.

[24] H. Binder, A. Kohling, K. Richter and G. Sandstede, *Electrochim. Acta* **9** (1964) 255.

[25] V. Sihvonen, *Trans Electrochem. Soc.* **34** (1938) 1062.

[26] K. Kinoshita, Proceedings of the Workshop on the Electrochemistry of Carbon, edited by S. Sarangapani, J. R. Akridge and B. Schumm, The Electrochemical Society, Pennington, New Jersey (1984) p. 273.

[27] L. J. J. Janssen, *Electrochim. Acta* **19** (1974) 257.

[28] F. Hine, M. Yasuda and M. Iwata, *J. Electrochem. Soc.* **121** (1974) 749.

[29] N. Giordano and A. Paratella, *Mem. Accademia Patavia di SS.LL.AA.* **78** (1966) 379.